

# A Measurement of the Muon Magnetic Moment Using Cosmic Rays

By

Daniel Atkinson Kroening

Submitted to the Department of Physics  
in partial fulfillment of the requirements for the degree of

Bachelor of Science

at

Houghton College

May 2002

Signature of Author.....

Department of Physics  
May 8, 2002

.....

Dr. Mark Yuly  
Associate Professor of Physics  
Research Supervisor

.....

Dr. Ronald Rohe  
Associate Professor of Physics

# A Measurement of the Muon Magnetic Moment Using Cosmic Rays

By

Daniel Atkinson Kroening

Submitted to the Department of Physics  
on 8 May 2002 in partial fulfillment of the  
requirements for the degree of  
Bachelor of Science

## Abstract

The muon magnetic moment was measured via the decay of polarized cosmic-ray muons in a constant magnetic field with a three-scintillator detector system. Cosmic-ray muons stop in the central detector, precess in the magnetic field, and then decay by emitting positrons along the muon spin axis. A quantum-mechanical calculation allows the g-factor to be extracted from a measurement of the number of positrons emitted into one direction as a function of decay time. The results are  $\tau = 2.28 \pm 0.07 \mu\text{s}$  (mean decay time) and  $g = 2.74 \pm 0.20$ . Some possible explanations for the large value of g are discussed.

Thesis Supervisor: Dr. Mark Yuly  
Title: Associate Professor of Physics

# Table of Contents

<b>Table of Figures .....</b>	<b>2</b>
<b>Introduction.....</b>	<b>3</b>
History.....	3
Test of Current Theories .....	4
Current Experiment.....	5
Cosmic Ray Muons as a Test of Relativity.....	6
<b>Setup and Experimental Procedure .....</b>	<b>8</b>
<b>Theory .....</b>	<b>10</b>
<b>Results .....</b>	<b>17</b>
<b>Conclusion .....</b>	<b>24</b>
<b>References.....</b>	<b>25</b>
<b>Appendix A.....</b>	<b>26</b>
Apparatus Diagrams.....	26
<b>Appendix B.....</b>	<b>28</b>
Data Taken With Magnetic Field Off.....	28
Data Taken With Magnetic Field On.....	31
<b>Appendix C.....</b>	<b>34</b>
Root Code Used for Plotting and Fitting Decay Curves.....	34

## Table of Figures

Figure 1: Polarization of positive cosmic ray muons.....	6
Figure 2: A simplified drawing of the experimental setup. ....	9
Figure 3: A diagram showing the precession of the muon spin.....	15
Figure 4: Best-fit of Eq. (34) from 2.1 $\mu\text{s}$ to 7.9 $\mu\text{s}$ . ....	21
Figure 5: Best-fit of Eq. (33) from 2.1 $\mu\text{s}$ to 7.9 $\mu\text{s}$ .....	21
Figure 6: Best-fit of Eq. (34) from 1.2 $\mu\text{s}$ to 7.9 $\mu\text{s}$ . ....	22
Figure 7: Best-fit of Eq. (33) from 1.2 $\mu\text{s}$ to 7.9 $\mu\text{s}$ .....	22
Figure 8: Best-fit of Eq. (34) from 0.2 $\mu\text{s}$ to 7.9 $\mu\text{s}$ . ....	23
Figure 9: Best-fit of Eq. (33) from 0.2 $\mu\text{s}$ to 7.9 $\mu\text{s}$ .....	23
Figure 10: Scale Drawing of Apparatus.....	26
Figure 11: Electronics Diagram.....	27

# Introduction

## History

In 1935 the Japanese physicist Hideki Yukawa predicted [1] the existence of the meson, a particle of intermediate mass that carries the strong force. The muon, discovered by Anderson and Nedermeyer [2] in 1937 with a mass of  $105 \text{ MeV}/c^2$ , was originally considered to be this same particle. It was later demonstrated, however, that the muon was unaffected by the strong force [3,4], necessitating further research. In 1947, Lattes et al. identified the pion [4], with a mass of about  $140 \text{ MeV}/c^2$ ; this particle did interact via the strong force, and has since been shown to be its long-range carrier. These findings supported Yukawa's meson prediction, and in 1949 he was awarded the Nobel Prize for his work. The term 'meson' has since been redefined as a particle consisting of two quarks rather than a particle of intermediate mass; and though the muon can no longer be characterized as a meson, a relationship to the pion does still exist. Pion decay will result in a muon and a muon neutrino 99.99% of the time [5], in the reaction:



Pion production (via high energy collisions of nucleons), and subsequent decay is the usual means for obtaining muons for experimental work.

The muon is a lepton—a fundamental particle with spin  $\frac{1}{2}$  that does not interact via the strong force but does interact via electromagnetic forces. Since it is a particle with spin, the muon has an intrinsic magnetic moment. The muon's magnetic moment is proportional to the gyromagnetic ratio (called  $g$ , the  $g$ -factor or the Landé factor) and is usually written in terms of it. Because the  $g$ -factor of the muon is near 2.0, the muon magnetic moment is usually reported in terms of

$$a_\mu \equiv \frac{g-2}{2}.$$

The muon magnetic moment was first measured in 1957 by R.L. Garwin [6]. This experiment measured the magnetic moment to 3 decimal places ( $2.00 \pm .010$ ). Subsequent measurements at CERN [7] in 1977 ( $2.0023318460 \pm .0000000168$ ) and at Brookhaven National Labs [8] from 1997-2002 ( $2.0023318404 \pm .0000000030$ ) have established precision out to eleven places.

## Test of Current Theories

The magnetic moment of the muon has been historically of great interest, in part because it is a sensitive test of quantum electrodynamics (QED). QED is a quantum field theory that is used to describe the interactions of leptons in an electromagnetic field. Because the muon is a lepton, and therefore interacts via electromagnetic forces, it will interact with a magnetic field. This interaction occurs in the form of precession, as the spin axis of the muon will rotate around the direction of the magnetic field lines. By measuring the rate of precession of the muon spin axis in the magnetic field a value for  $a_\mu$  may be found, and a comparison with the value predicted using QED can be made.

The Standard Model, which is currently considered to be the best model for describing particles and their interactions, includes 12 fundamental spin  $\frac{1}{2}$  particles—six quarks and six leptons (of which  $\mu^-$  is one), and their anti-particles ( $\mu^+$  included). It describes particle interactions with four forces (strong, weak, electromagnetic and gravitational), all of which have mediating particles. Because a prediction using QED is based on the assumptions of the Standard Model, a difference between experimental and theoretically predicted values for the muon magnetic moment could potentially indicate either a problem with the Standard Model or with QED. Current results for the experimental and predicted values of  $a_\mu$  are:

$$a_\mu(\text{exp}) = 11659202(14)(6) \times 10^{-10} [8].$$

$$a_\mu(\text{theory}) = 11659159.7(6.7) \times 10^{-10} [9].$$

While these two values are 2.6 standard deviations apart, there are many who believe it is due to a miscalculation in the theoretical value [10], rather than a fundamental error in the Standard Model itself [9]. A recent publication by M. Hayakawa and T. Kinoshita [11] found a sign error in the Standard Model prediction which, when corrected, brings the values of  $a_\mu$  within 1.6 standard deviations of the experimental value.

## Current Experiment

Our current experiment utilizes a tabletop apparatus similar to the one described by Amsler [12], to measure  $a_\mu$  of cosmic ray muons. Cosmic ray muons are created in the upper atmosphere by the decay of mesons (primarily pions) produced in high-energy collisions of nucleons in the upper atmosphere. A falling pion may emit a muon either forward or backward in its own frame. In the lab frame a muon emitted backward will have a spin parallel to its own direction of flight, and a muon emitted forward will have spin antiparallel. Since by energy conservation a muon of a given energy may be produced by forward emission from a pion of one energy ( $E_1$ ) or backward emission from a pion of a greater energy ( $E_2$ ), the net polarization of muons with this energy will be zero only if there are an equal number of pions with energies  $E_1$  and  $E_2$ . Because pion production is not uniform over all energies, the result is a non-zero polarization of the cosmic ray muon, as shown in Figure 1—a measurement of the polarization of  $\mu^+$  from the paper by Amsler [12].

Because they have a magnetic moment, muons in a magnetic field with a component perpendicular to their spin axis will begin to precess. Since the incident muons have a net polarization, the average muon spin direction will be pointed preferentially in a given direction for any given time. Muons decay primarily with the emission of a positron or electron and two neutrinos as shown [5]:

$$\mu^+ \rightarrow e^+ + \nu_e + \bar{\nu}_\mu, \text{ or}$$

$$\mu^- \rightarrow e^- + \nu_\mu + \bar{\nu}_e.$$

Because the positron or electron is emitted antiparallel to the parent muon's spin direction, detection of the decay direction will indicate the muon's spin direction at the time of decay. By recording the muon decay time while in the field, it was possible to keep track of their spin as a function of time, and to consequently measure their magnetic moment.

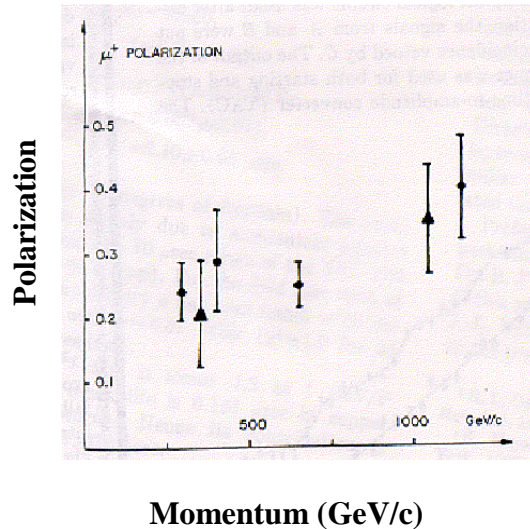


**Figure 1:** Plot of the polarization of positive cosmic ray muons with varying momenta. From the paper by C. Amsler [12].

## Cosmic Ray Muons as a Test of Relativity

A similar experimental apparatus [13] has been used at an undergraduate level as a demonstration of special relativity, and has been used to explore relativistic effects such as time dilation and length contraction. Cosmic ray muons have a nearly constant energy when moving in the atmosphere, making their velocity virtually constant throughout their descent. By triggering only on a small range of velocities, then, issues of acceleration and general relativity are avoided. According to special relativity, lifetime measurements in the lab frame and the muon rest frame will be significantly different. By measuring the difference in flux of muons at various altitudes (e.g. sea level, and on a mountain), the percentage of muons at the higher altitude that decay before reaching the lower altitude



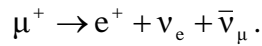
can be found. Utilizing the well-known mean lifetime of the muon ( $2.19 \mu\text{s}$ ), one may calculate the time lapse that the muon observed in traversing the distance between the two altitudes. A comparison of this time to that observed in the lab frame makes demonstration of the effects of special relativity possible.

## Setup and Experimental Procedure

An experiment was conducted to measure the magnetic moment of the muon. The lifetimes of muons were recorded as their spins precessed in a  $42 \pm 2$  G magnetic field created by a hand-wound solenoid. Inside the solenoid were three large, rectangular plastic scintillator detectors, which output a flash of light upon incidence of a charged particle. Light emissions were converted to electrical pulses by a photomultiplier tube (PMT) attached to a scintillator. A fourth detector was placed above the solenoid to veto events from parts of the detectors in a region of non-uniform field.

A simplified diagram of the experimental setup is shown in Figure 2 (a more detailed diagram may be found in App. A). The purpose of the apparatus was to measure the time difference between the stopping of a muon in the central detector and its subsequent decay. If scintillator 1 and 2 both detected an event, but not scintillator 3, a muon must have stopped in the center detector, so the timer was started. Subsequently, if scintillators 2 and 3 triggered, but not scintillator 1, a decay positron must have emitted downward, and the timer was stopped. The time difference between these coincidences was measured by a Time to Amplitude Converter (TAC)—a device that measures the time between two input signals, then outputs an analog pulse with pulse height proportional to the time difference. This time difference was the decay time of the muon. The output of the TAC was sent to a Multi-Channel Analyzer (MCA), a device that sorts the input pulses by pulse height into different ‘bins’, or channels, for the purpose of making a histogram. The TAC and MCA were calibrated by sending pulses at known time intervals to the TAC from a gate generator; the bin numbers to which each time interval corresponded was then recorded.

Since  $\mu^-$  behave similarly to electrons, these particles are commonly ‘trapped’ by elements within the apparatus and left to fill the inner shell of an atom, forming ‘muonium’[14]. The large overlap of the muon and nucleus wavefunction results in an increased probability of muon decay, and hence a much shorter mean-lifetime for the captured  $\mu^-$ , on the order of 100 ns [14], as opposed to 2.19  $\mu$ s for a free muon. By excluding lifetimes shorter than this, it was assured that the only decay particles that were recorded were positrons from the reaction:



Because the muon's spin generally had a component perpendicular to the magnetic field, the spin precessed at a rate proportional to the field strength. Since only coincidences between the second and third detector were used to stop the TAC, the lifetimes of muons whose spins were pointing up at the time of decay were recorded, but not those whose spins were pointing down, since positrons are emitted antiparallel to the spin. If the TAC did not receive a stop signal within 20  $\mu\text{s}$ , it reset. Since the muon's spin precessed at a constant rate, more events were recorded for certain lifetimes—events corresponding to muon decay into a positron that hit scintillator 3. This caused the decay curve for the muon to have an added sinusoidal component, making measurement of the magnetic moment possible.

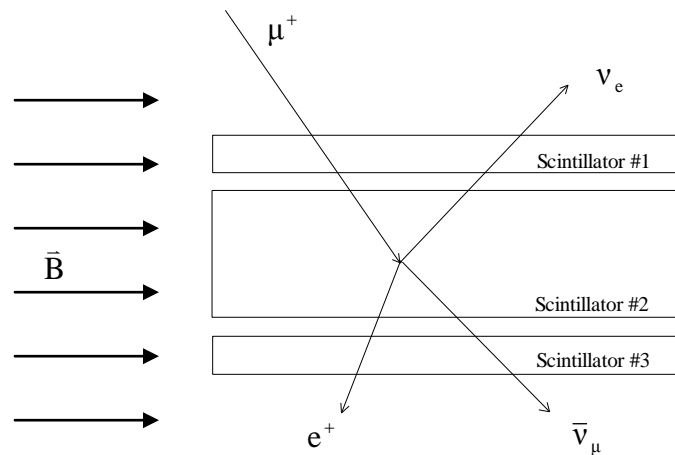


**Figure 2:** A simplified drawing of the experimental setup. A positive muon deposited energy in scintillator 1 and stopped in scintillator 2. The muon's spin precessed about the axis of the magnetic field  $\vec{B}$  until it decayed into a positron and two neutrinos. A positron detected by the lower scintillator indicated that the muon's spin was pointing upwards at the time of decay.

## Theory

Classically the spin axis of the muon precesses around in the magnetic field. When examined using quantum mechanics however, it is found that it is the expectation value of the spin direction that is precessing. Of course, for a spin- $1/2$  particle, only two spin states are allowed, so each muon individually has only two allowed directions for the magnetic moment.

The expectation value of the spin of the muon may be determined following an argument similar to the one presented by Townsend [15]. The Hamiltonian, or energy operator, may be written in terms of the magnetic moment operator such that

$$\hat{H} = -\hat{\boldsymbol{\mu}} \cdot \bar{\mathbf{B}}, \quad (1)$$

$$\text{where, } \hat{\boldsymbol{\mu}} = \frac{gq\hat{\mathbf{S}}}{2mc}.$$

In the expressions  $\hat{\mathbf{S}}$  is the intrinsic spin operator,  $m$  is the mass of the muon,  $q$  is its charge,  $g$  is the Landé factor of the muon, and the magnetic field is  $\bar{\mathbf{B}}$ . If  $\bar{\mathbf{B}}$  is constant and along the  $z$ -axis ( $\bar{\mathbf{B}} = B_z \hat{\mathbf{k}}$ ), then the dot product of the spin operator and magnetic field leaves only the  $z$ -component of the spin operator.

$$\hat{H} = \frac{-gq\hat{\mathbf{S}} \cdot \bar{\mathbf{B}}}{2mc} = \frac{-gq\hat{S}_z B_z}{2mc}. \quad (2)$$

Hence,

$$\hat{H} = \omega \hat{S}_z, \quad (3)$$

where  $\omega = \frac{-gqB_z}{2mc}$  is the precession frequency, which will be discussed later.

Since the Hamiltonian is proportional to the intrinsic spin operator in the  $z$ -direction, the two operators will have the same eigenstates. The eigenvalues for  $\hat{S}_z$  are  $\pm \hbar/2$ , so

$$\hat{H} |\pm \mathbf{z}\rangle = \omega \hat{S}_z |\pm \mathbf{z}\rangle = \pm \omega (\hbar/2) |\pm \mathbf{z}\rangle \quad (4)$$

where  $\pm \hbar \omega/2$  are the energy eigenvalues for the  $|\pm \mathbf{z}\rangle$  and  $|\pm \mathbf{x}\rangle$  eigenstates.

Assume that the muon that enters the center scintillator is in the  $|\pm \mathbf{x}\rangle$  state. At  $t=0$ , then,

$$|\psi(0)\rangle \equiv |\pm \mathbf{x}\rangle = \left( \frac{|+\mathbf{z}\rangle}{\sqrt{2}} + \frac{|-\mathbf{z}\rangle}{\sqrt{2}} \right). \quad (5)$$

This state will evolve according to the time-evolution operator,  $\hat{U}(t) = e^{-i\hat{H}t/\hbar}$ , so that the particle, at time  $t$ , will be in the state

$$|\psi(t)\rangle = e^{-i\hat{H}t/\hbar} \left( \frac{|+\mathbf{z}\rangle}{\sqrt{2}} + \frac{|-\mathbf{z}\rangle}{\sqrt{2}} \right). \quad (6)$$

Since  $\hat{H} |\pm \mathbf{z}\rangle = \pm (\hbar \omega/2) |\pm \mathbf{z}\rangle$ , it can be shown that

$$|\psi(t)\rangle = \left( \frac{e^{i\omega t/2} |+\mathbf{z}\rangle}{\sqrt{2}} + \frac{e^{-i\omega t/2} |-\mathbf{z}\rangle}{\sqrt{2}} \right). \quad (7)$$

The probability of finding the muon in the  $|\pm \mathbf{z}\rangle$  and  $|\pm \mathbf{x}\rangle$  states are therefore,

$$\langle +\mathbf{z} | \psi(t) \rangle^2 = \left| \frac{e^{i\omega t/2}}{\sqrt{2}} \right|^2 = 1/2 \quad (8)$$

and

$$\langle -\mathbf{z} | \psi(t) \rangle^2 = \left| \frac{e^{-i\omega t/2}}{\sqrt{2}} \right|^2 = 1/2. \quad (9)$$

Thus the probability that the energy is  $\hbar\omega/2$  is  $1/2$  and  $-\hbar\omega/2$  is also  $1/2$ ; these are constant in time. We may also find the probability that the muon will be in the  $|+\mathbf{x}\rangle$  or  $|-\mathbf{x}\rangle$  states.

$$\langle +\mathbf{x} | \psi(t) \rangle = \left( \frac{\langle +\mathbf{z} |}{\sqrt{2}} + \frac{\langle -\mathbf{z} |}{\sqrt{2}} \right) \left( \frac{e^{i\omega t/2} |+\mathbf{z}\rangle}{\sqrt{2}} + \frac{e^{-i\omega t/2} |-\mathbf{z}\rangle}{\sqrt{2}} \right) \quad (10)$$

This reduces to

$$\langle +\mathbf{x} | \psi(t) \rangle = \left( \frac{e^{i\omega t/2}}{2} + \frac{e^{-i\omega t/2}}{2} \right) = \cos\left(\frac{\omega t}{2}\right), \quad (11)$$

The probability of finding the muon in the  $|+\mathbf{x}\rangle$  state is therefore

$$|\langle +\mathbf{x} | \psi(t) \rangle|^2 = \cos^2\left(\frac{\omega t}{2}\right). \quad (12)$$

The probability of finding the particle in the  $|-\mathbf{x}\rangle$  state can be arrived at similarly:

$$|-\mathbf{x}\rangle = \left( \frac{|+\mathbf{z}\rangle}{\sqrt{2}} - \frac{|-\mathbf{z}\rangle}{\sqrt{2}} \right), \quad (13)$$

therefore

$$\langle -\mathbf{x} | \psi(t) \rangle = \left( \frac{\langle +\mathbf{z} |}{\sqrt{2}} - \frac{\langle -\mathbf{z} |}{\sqrt{2}} \right) \left( \frac{e^{i\omega t/2} |+\mathbf{z}\rangle}{\sqrt{2}} + \frac{e^{-i\omega t/2} |-\mathbf{z}\rangle}{\sqrt{2}} \right) \quad (14)$$

$$\langle -\mathbf{x} | \psi(t) \rangle = \left( \frac{e^{i\omega t/2}}{2} - \frac{e^{-i\omega t/2}}{2} \right) = \sin\left(\frac{\omega t}{2}\right) \quad (15)$$

$$|\langle -\mathbf{x} | \psi(t) \rangle|^2 = \sin^2\left(\frac{\omega t}{2}\right). \quad (16)$$

Note that these probabilities are time dependent, unlike the probabilities of the particle being in  $|\pm\mathbf{z}\rangle$ . The expectation value of the x-component of the spin is the sum of the two eigenvalues, multiplied by their respective probabilities:

$$\langle \hat{S}_x \rangle = \left(\frac{\hbar}{2}\right) \cos^2\left(\frac{\omega t}{2}\right) + \left(\frac{-\hbar}{2}\right) \sin^2\left(\frac{\omega t}{2}\right) = \frac{\hbar}{2} \cos(\omega t). \quad (17)$$

The average value of  $\hat{S}_y$  can be found similarly. We know that

$$|+\mathbf{y}\rangle = \left(\frac{|+\mathbf{z}\rangle}{\sqrt{2}} + \frac{i|-\mathbf{z}\rangle}{\sqrt{2}}\right), \quad (18)$$

and the complex conjugate is:

$$\langle +\mathbf{y} | = \left(\frac{\langle +\mathbf{z} |}{\sqrt{2}} - \frac{i\langle -\mathbf{z} |}{\sqrt{2}}\right). \quad (19)$$

Therefore

$$\langle +\mathbf{y} | \psi(t) \rangle = \left(\frac{\langle +\mathbf{z} |}{\sqrt{2}} - \frac{i\langle -\mathbf{z} |}{\sqrt{2}}\right) \left(\frac{e^{i\omega t/2} |+\mathbf{z}\rangle}{\sqrt{2}} + \frac{e^{-i\omega t/2} |-\mathbf{z}\rangle}{\sqrt{2}}\right) \quad (20)$$

$$\langle +\mathbf{y} | \psi(t) \rangle = \left(\frac{e^{-i\omega t/2}}{2} - \frac{ie^{i\omega t/2}}{2}\right). \quad (21)$$

The probability of finding the muon in the  $|+\mathbf{y}\rangle$  state may be found:

$$|\langle +\mathbf{y} | \psi(t) \rangle|^2 = \langle +\mathbf{y} | \psi(t) \rangle^* \langle +\mathbf{y} | \psi(t) \rangle = \left(\frac{e^{i\omega t/2}}{2} + \frac{ie^{-i\omega t/2}}{2}\right) \left(\frac{e^{-i\omega t/2}}{2} - \frac{ie^{i\omega t/2}}{2}\right) \quad (22)$$

Therefore

$$\left| \langle +\mathbf{y} | \psi(t) \rangle \right|^2 = \frac{1}{2} - \frac{i(e^{i\omega t} - e^{-i\omega t})}{4} = \frac{1 + \sin(\omega t)}{2}. \quad (23)$$

The probability of the  $|-\mathbf{y}\rangle$  state can be arrived at similarly:

$$|-\mathbf{y}\rangle = \left( \frac{|+\mathbf{z}\rangle}{\sqrt{2}} - \frac{i|-\mathbf{z}\rangle}{\sqrt{2}} \right), \quad (24)$$

and the complex conjugate is:

$$\langle -\mathbf{y} | = \left( \frac{\langle +\mathbf{z} |}{\sqrt{2}} + \frac{i\langle -\mathbf{z} |}{\sqrt{2}} \right). \quad (25)$$

Therefore,

$$\langle -\mathbf{y} | \psi(t) \rangle = \left( \frac{\langle +\mathbf{z} |}{\sqrt{2}} + \frac{i\langle -\mathbf{z} |}{\sqrt{2}} \right) \left( \frac{e^{i\omega t/2} |+\mathbf{z}\rangle}{\sqrt{2}} + \frac{e^{-i\omega t/2} |-\mathbf{z}\rangle}{\sqrt{2}} \right) \quad (26)$$

$$\langle -\mathbf{y} | \psi(t) \rangle = \left( \frac{e^{-i\omega t/2}}{2} + \frac{ie^{i\omega t/2}}{2} \right). \quad (27)$$

The probability of finding the muon in the  $|-\mathbf{y}\rangle$  state may be found:

$$\left| \langle -\mathbf{y} | \psi(t) \rangle \right|^2 = \langle -\mathbf{y} | \psi(t) \rangle^* \langle -\mathbf{y} | \psi(t) \rangle = \left( \frac{e^{i\omega t/2}}{2} - \frac{ie^{-i\omega t/2}}{2} \right) \left( \frac{e^{-i\omega t/2}}{2} + \frac{ie^{i\omega t/2}}{2} \right) \quad (28)$$

Therefore

$$\left| \langle +\mathbf{y} | \psi(t) \rangle \right|^2 = \frac{1}{2} + \frac{i(e^{i\omega t} - e^{-i\omega t})}{4} = \frac{1 - \sin(\omega t)}{2}. \quad (29)$$



The expectation value of the y-component of the spin is the sum of the two eigenvalues multiplied by their respective expectation values:

$$\langle \hat{S}_y \rangle = \left( \frac{\hbar}{2} \right) \left( \frac{1 - \sin(\omega t)}{2} \right) + \left( \frac{-\hbar}{2} \right) \left( \frac{1 - \sin(\omega t)}{2} \right). \quad (30)$$

$$\langle \hat{S}_y \rangle = \frac{\hbar}{2} \sin(\omega t). \quad (31)$$

Therefore, the magnitude of the component of spin in the x-y plane is

$$\sqrt{\langle \hat{S}_x \rangle^2 + \langle \hat{S}_y \rangle^2} = \frac{\hbar}{2} \sqrt{\cos^2(\omega t) + \sin^2(\omega t)} = \frac{\hbar}{2}. \quad (32)$$

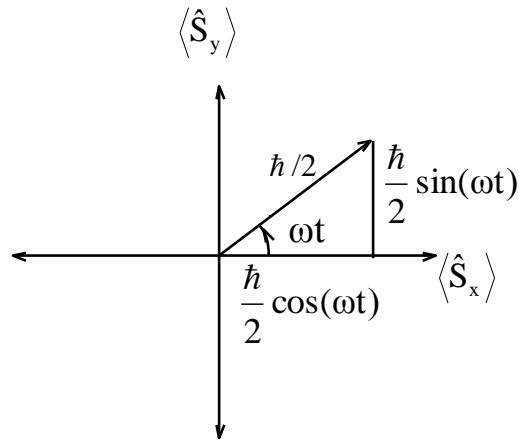


**Figure 3:** A diagram showing the precession of the muon spin. The expectation value of the muon will precess with angular frequency  $\omega$ . The magnitude of the expectation value for the spin is  $\hbar/2$ .

The spin expectation values may be physically interpreted as in Fig. 3, where  $\langle \hat{S}_x \rangle$  is the x-component of the expectation value of the spin, while  $\langle \hat{S}_y \rangle$  is the y component. These components vary with time based on angle  $\omega t$ , where  $\omega$  may therefore be interpreted as the angular frequency of precession. Thus, the expectation value of the spin vector precesses just as the classical angular momentum would.

Our apparatus is capable of detecting  $\mu^+$  that stop in the center detector and the subsequent decay positron if ejected downward. Because the decay positron will preferentially eject anti-parallel to the spin of the parent muon, the data collected will be asymmetrical, favoring decays where the spin of the muon was upward. This asymmetry, which fluctuates with time, will cause the sinusoidal behavior of Eq. (31) to be superimposed on the normal decay curve. In the absence of a magnetic field, the decay rate is given by,

$$R(t) = R_0 e^{-\frac{t}{\tau}} + B, \quad (33)$$

where  $\tau$ , the mean lifetime, has been measured to be about  $2.19 \mu\text{s}$  [5].  $R(t)$  is the decay rate at time  $t$ ,  $R_0$  is the rate at  $t = 0$ , and  $B$  accounts for background due to accidental coincidences. Such accidental coincidences will occur at random times, and may be accounted for in the curve fit with a constant. Including the sinusoidal variations due to precession into the decay rate equation gives:

$$R(t) = R_0 e^{-\frac{t}{\tau}} (1 + A \sin(\omega t + \delta)) + B. \quad (34)$$

In this equation  $\delta$  is a phase shift to account for the initial spin state of the muon.  $A$  accounts for the polarization of incident muons. In the case of 100% polarization,  $A$  would be one, causing the sin term to fluctuate from negative one to positive one. Consequently, at certain times,  $R(t)$  would equal  $B$ , indicating that no decay particles were ejected downward.

## Results

Equations (33) and (34) were fit to the data in order to determine the  $\mu^+$  magnetic moment. Data were collected with the magnetic field from September 20, 2001 through December 6, 2001 (78 days); 67,593 events were recorded. Data were also collected without the field from December 7, 2001 through February 5, 2002 (60 days); 67,329 events were recorded. These data can be found in Appendix B.

Muon decay times under 10  $\mu\text{s}$  were recorded in 486 bins in the MCA, but these were re-binned at a ratio of 10:1 for final data analysis in order to reduce the statistical uncertainty of each point while maintaining a sufficient amount of data points for a curve fit. The first ten bins were not used in the fit; as they represented the first 190 ns, corresponding to the period over which most of the  $\mu^-$  would decay.

Eq. (34) from the theory section was fit to the data, and statistical uncertainty values were obtained using the function minimization program, Minuit [16]. The C++ based program, ROOT [17], was used for plotting. The value  $\chi^2$  was used to describe the closeness of the fit, and is defined as:

$$\chi^2 = \sum_i^m \frac{(f(a_j, t_i) - y_i)^2}{(\sigma_i)^2}. \quad (35)$$

$m$  is the number of data points being fit,  $n$  is the number of parameters in the equation being fit to the data,  $t$  is the independent time variable, and  $y$  is the value of a data point.  $\sigma$  is the statistical uncertainty of  $y$ , and is  $\sqrt{y}$  in this case. The value of  $\chi^2$  per degree of freedom is used to compare the quality of fits, being minimized for a best fit; it is defined as  $\chi^2$  divided by the number of data points minus the number of parameters.

Minuit used the  $\chi^2$  per degree of freedom to calculate the uncertainty in all of the parameters. Around the minimum value of  $\chi^2$  per degree of freedom will be a range of values which are less than or equal to one plus this minimum value. The uncertainty of any parameter is defined as one half the width of the domain that maps to this range. The precession frequency uncertainty was found using this method. The precession frequency,  $\omega$ , had different values for any given decay time range the data was analyzed over. Table

1 shows data taken with the field on. Corresponding figure numbers with their best-fit curve lines are indicated, as well as  $\chi^2$  per degree of freedom for that fit.

**Table 1:** Angular frequency values and uncertainties over varying time ranges used in the fit.

Bin Range	Time Range ( $\mu\text{s}$ )	$\omega$ ( $\mu\text{s}^{-1}$ )	$\delta\omega$ ( $\mu\text{s}^{-1}$ )	$\chi^2$ per degree of freedom	Figure #
110-410	2.13-7.94	4.87	$\pm.25$	.8148	Figure 4
60-410	1.16-7.94	5.13	$\pm.14$	.8699	Figure 6
10-410	.19-7.94	5.25	$\pm.12$	1.031	Figure 8

The fluctuation in the magnetic field was measured  $\pm 5\%$ , and this value was used as the uncertainty. The uncertainty in the other parameters [Table 2] was much smaller and was therefore neglected.

**Table 2:** Various parameters and their uncertainties.

Parameter	Value	Uncertainty
B	42.1 (G)	$\pm 1.7$ (G)
$q_\mu$	$1.6022 \times 10^{-19}$ (C)	
$m_\mu$	105.658432 (MeV/c <sup>2</sup> )	$\pm .000034$ (MeV/c <sup>2</sup> )

With these values g was found by using:

$$g = \frac{2m\omega}{qB}. \quad (36)$$

Uncertainty in g was obtained using propagation of errors, which yields the results, seen in Table 3.

**Table 3:** Experimental values of g and mean lifetime with uncertainties over varying ranges of muon lifetimes.

Bin Range	Time Range ( $\mu\text{s}$ )	g	$\tau$ ( $\mu\text{s}$ )
110-410	2.13-7.94	$2.74 \pm .20$	$2.28 \pm .07$
60-410	1.16-7.94	$2.89 \pm .16$	$2.19 \pm .04$
10-410	.19-7.94	$2.99 \pm .16$	$2.12 \pm .03$

It is interesting to note that none of our measured  $g$  values fall within error bars of previous experimental or theoretical values, though the range with the best  $\chi^2$  per degree of freedom (bins 110-410; 2.13-7.94  $\mu\text{s}$ ) is the closest. The central range (bins 60-410; 1.16-7.94  $\mu\text{s}$ ) has the closest value to the previously measured mean lifetime for a muon,  $2.19703 \pm .00004 \mu\text{s}$  [5].

This analysis does not include any systematic effects. There are some possible reasons for the disagreement in  $g$ -value that may give insight into the problem. For one, the magnetic field was irregular. Because the muons in areas of the solenoid with a weaker field will precess slower than in areas with stronger field, they cause the overall precession rate to be a blurred average of the precession rate in individual field regions. During earlier lifetimes, muons in all fields will have similar polarization. As time progresses, though, the individual precession frequencies will cause the polarizations to diverge, increasing the blurring. While the uncertainty in the magnetic field has been taken into account, the effect of multiple precession frequencies on the final curve, especially at large lifetimes, is unaccounted for.

All measurements of the magnetic field were made without the presence of the scintillators, and it is therefore possible that there was more uncertainty in the field than was accounted for. Measurements of the field with the scintillators present were not possible, however, as a hall-probe could not be inserted into the detector.

Another possible source of systematic uncertainty is the calibration of the Time to Amplitude Converter may have drifted over the six-month period of data acquisition. Calibration data from September 7, 2001 and February 15, 2002 indicate that the total drift was one bin, or 19 ns, between these dates. This difference is not significant enough to account for the disagreement in the  $g$  value. Also, the measured mean lifetime of the muon would have been affected as much as  $g$  had there been a significant drift; this was not the case.

Another possibility is that the effects of negatively charged muons are more significant than expected. While the first 10 channels were not used in order to avoid the possibility of extra counts that would be due to  $\mu^-$  decays, it is possible that this was not enough. While a check of Table 1 shows that an analysis of bins after 110 gives a far better fit than from before bin 110 ( $\sim 2.13 \mu\text{s}$ ), it is interesting to note that the value of  $\tau$  is

the farthest from previously measured values. This indicates that  $\mu^-$  decay was not completely responsible for the large value of  $g$ , if at all.

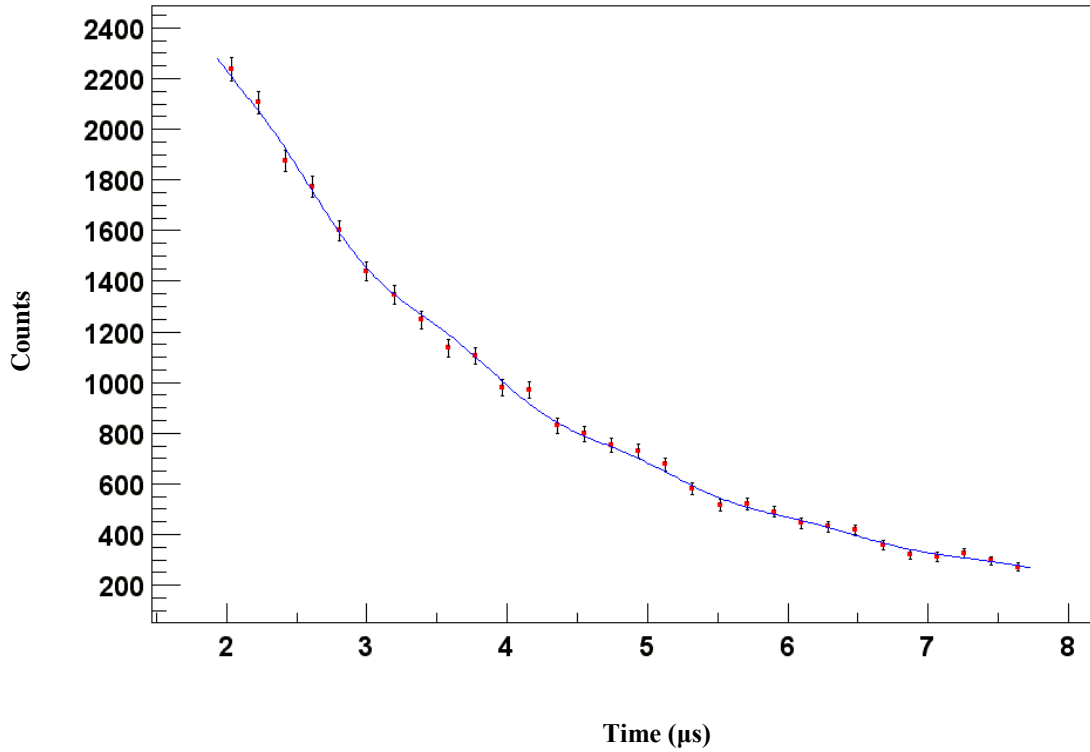


**Figure 4:** Best-fit of Eq. (34) to data from 2.1  $\mu\text{s}$  to 7.9  $\mu\text{s}$  (bins 110-410). Data were taken while the magnetic field was on. Note that zero is suppressed.

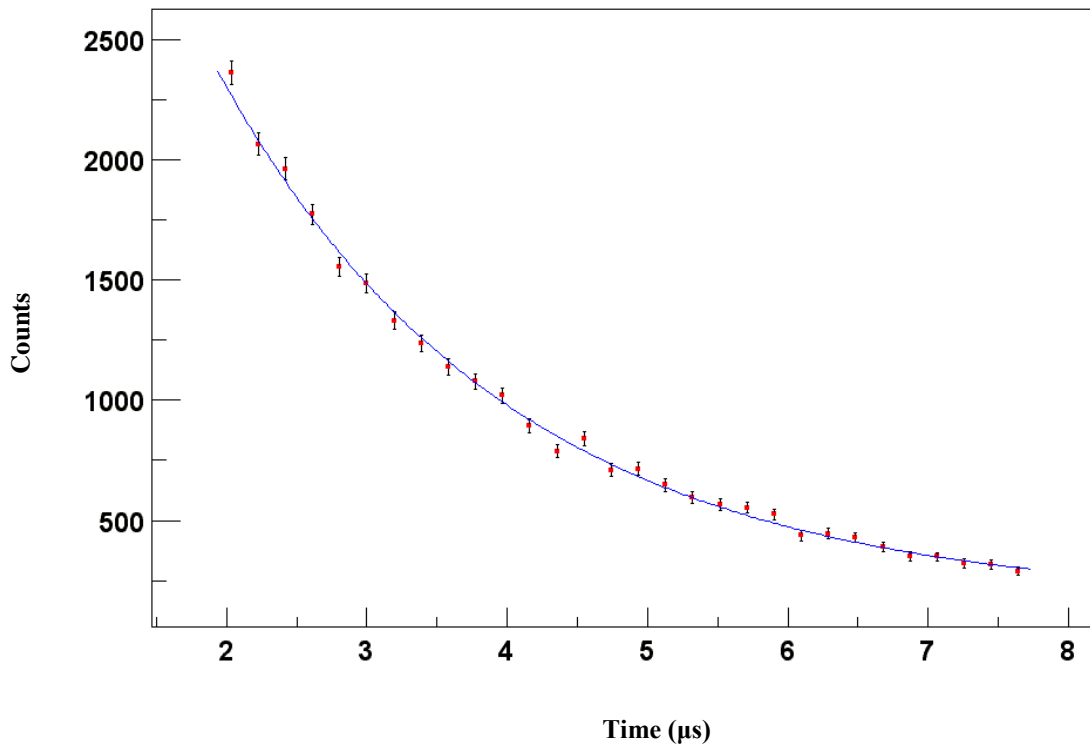


**Figure 5:** Best-fit of Eq. (33) to data from 2.1  $\mu\text{s}$  to 7.9  $\mu\text{s}$  (bins 110-410). Data were taken while the magnetic field was off. Note that zero is suppressed.

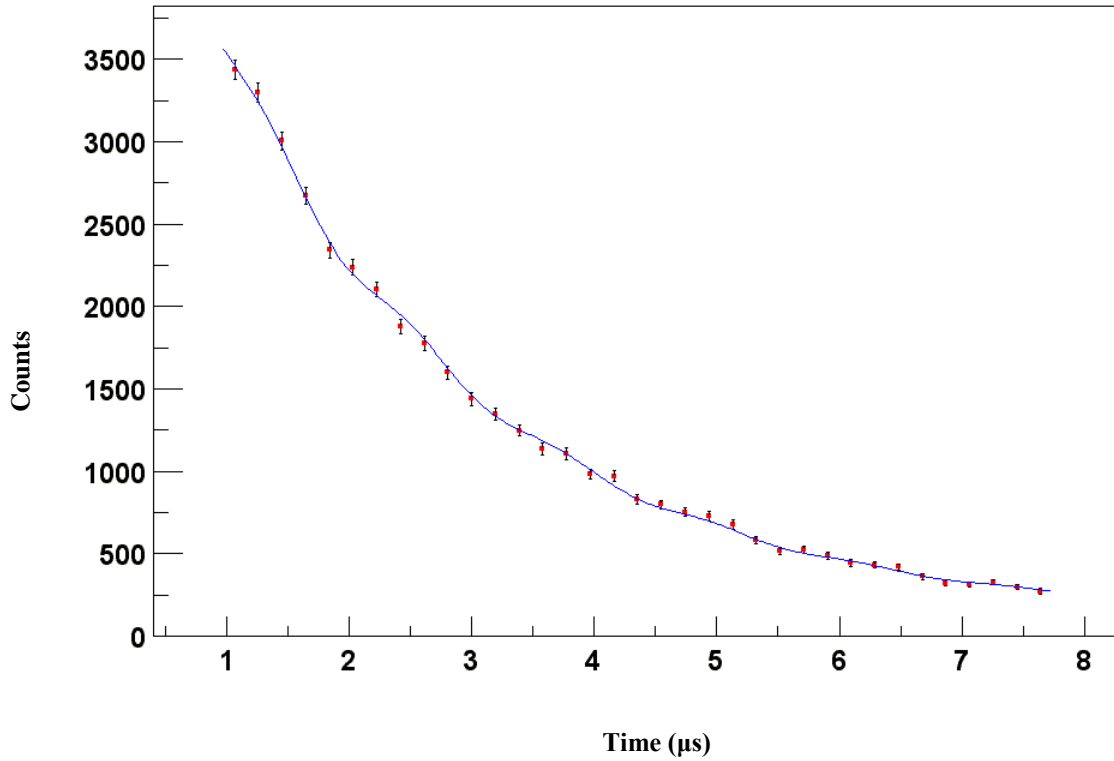


**Figure 6:** Best-fit of Eq. (34) to data from 1.2  $\mu\text{s}$  to 7.9  $\mu\text{s}$  (bins 60-410). Data were taken while the magnetic field was on. Note that zero is suppressed.

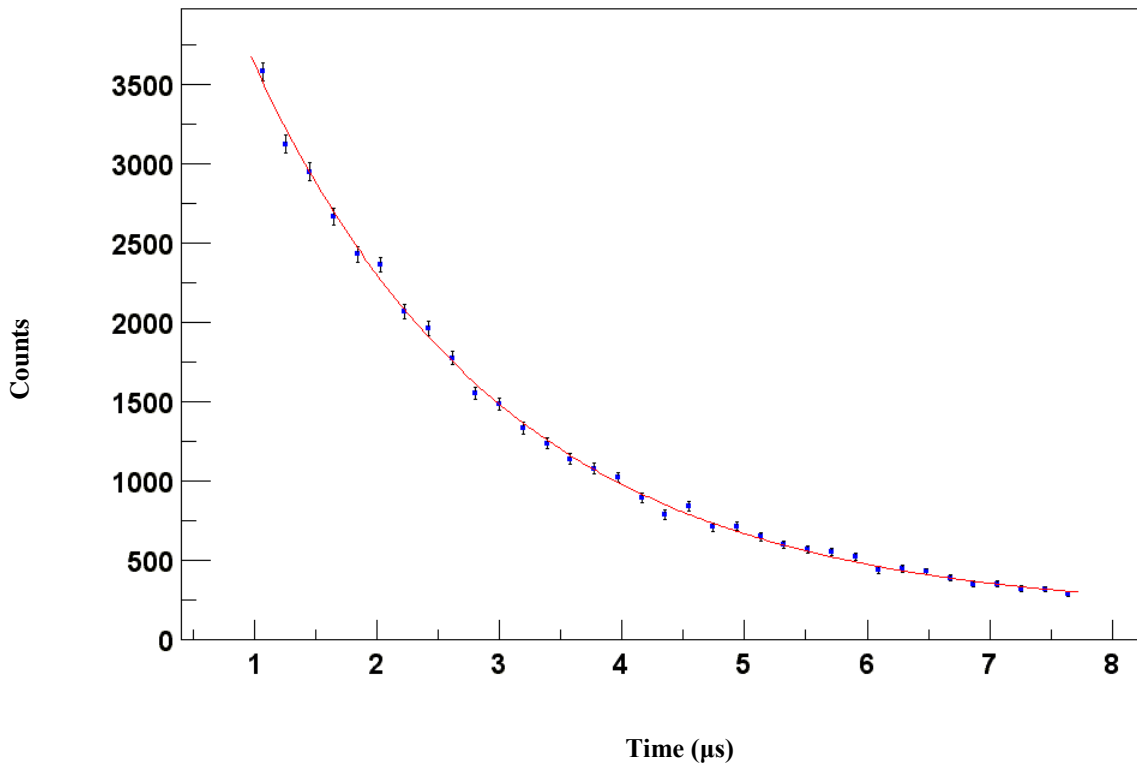


**Figure 7:** Best-fit of Eq. (33) to data from 1.2  $\mu\text{s}$  to 7.9  $\mu\text{s}$  (bins 60-410). Data were taken while the magnetic field was off. Note that zero is suppressed.



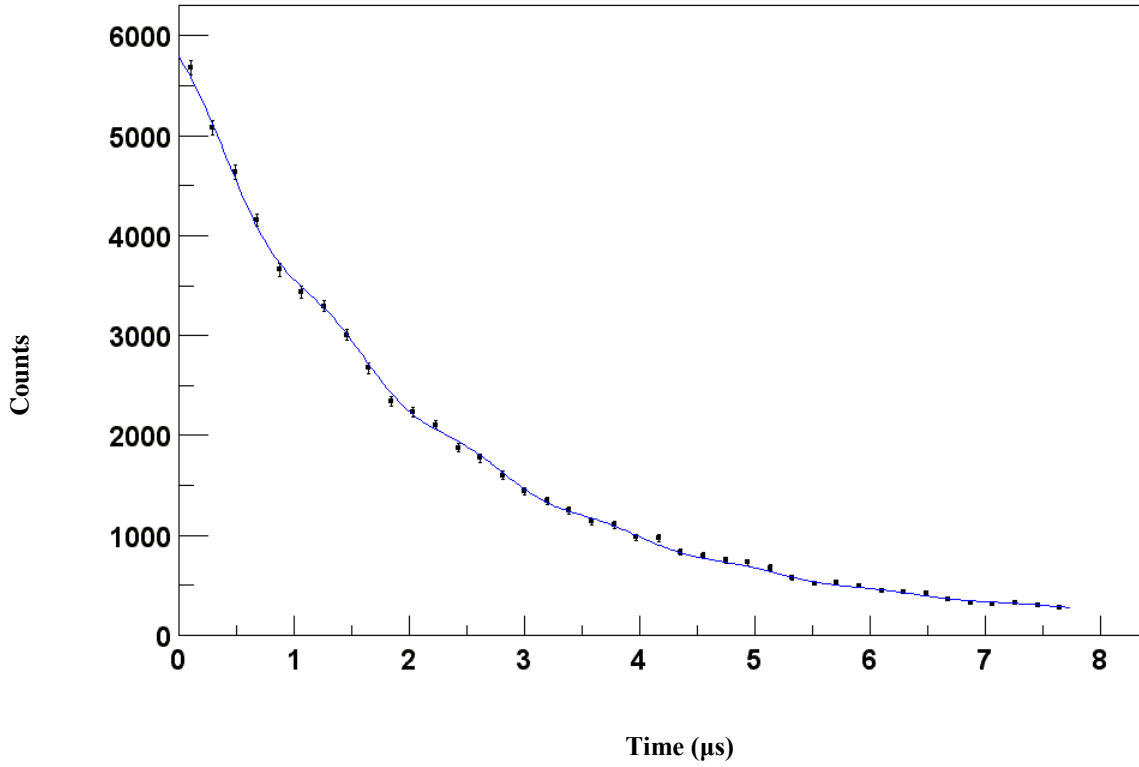


**Figure 8:** Best-fit of Eq. (34) to data from .2 μs to 7.9 μs (bins 10-410). Data were taken while the magnetic field was on.

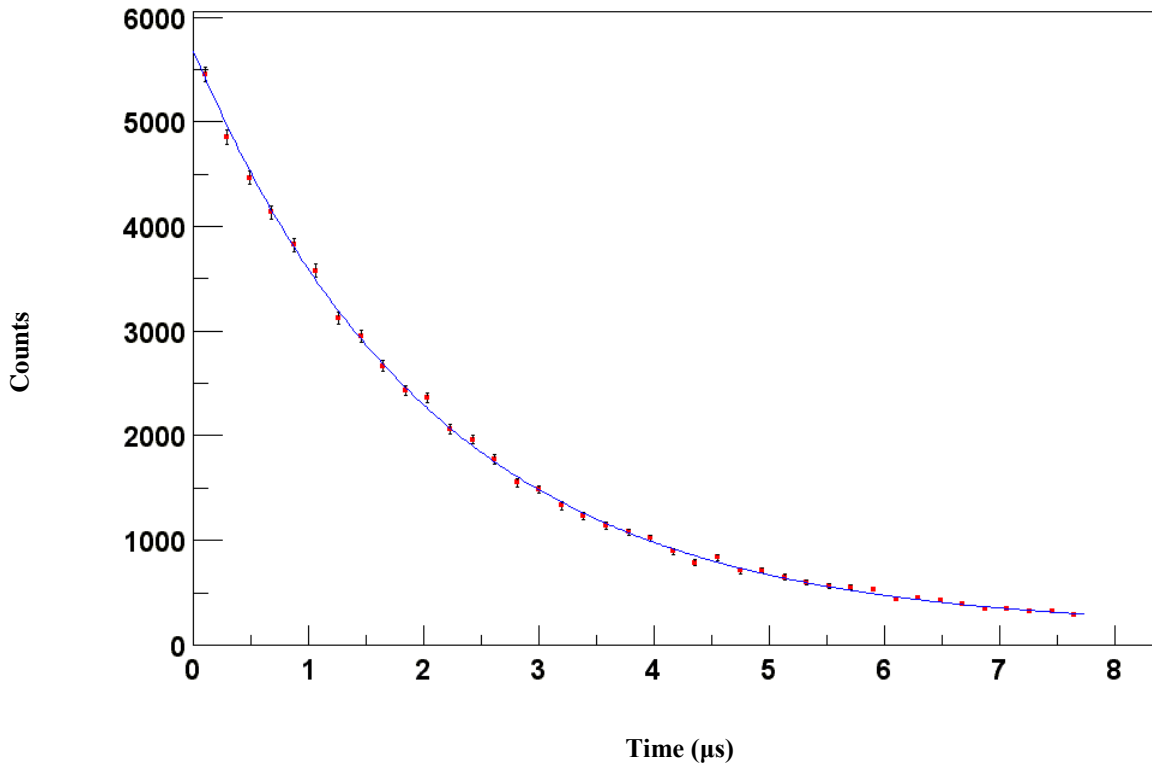


**Figure 9:** Best-fit of Eq. (33) to data from .2 μs to 7.9 μs (bins 10-410). Data were taken while the magnetic field was off.

## Conclusion

Using cosmic ray muons, the muon magnetic moment was measured inside a hand wound solenoid, which produced a magnetic field of  $42.1 \pm 1.7$  G. Three plastic scintillator detectors in the field were used to measure the decay times of precessing muons. A quantum-mechanical calculation allowed the g-factor to be extracted from these data. The results are  $\tau = 2.28 \pm 0.07$   $\mu\text{s}$  (mean decay time) and  $g = 2.74 \pm 0.20$ .

The results of this experiment indicate that muons were stopping and decaying in our setup, and that precession was occurring in the magnetic field. The sinusoidal variation of the decay curve indicates this. However, while our results for the mean lifetime of the muon are near previous measurements, there is disagreement between our value of g, which was  $2.74 \pm 0.20$  and the world average experimental value of  $2.0023318404 \pm .0000000030$  [8]. Our largest source of uncertainty, the magnetic field produced by our solenoid, does not seem to account for all of this disagreement.

It is possible that  $\mu^-$  decay may account for this disagreement. Because the theoretical model used to extract g only assumed that a  $\mu^+$  would stop in the magnetic field and begin to precess, the effects of  $\mu^-$  decay are not included. A  $\mu^-$  may react with atoms within the apparatus and have a greatly shortened lifetime as a result (19 ns versus 2.19  $\mu\text{s}$ ). This would affect the measurements made of the muon lifetime and magnetic moment.

In order to improve the experiment for the future, a more accurate mapping of a more constant magnetic field should be made. Given the solenoid used for this experiment, it would have been helpful for uncertainty analysis to know how the magnetic field behaved inside of the scintillators, as opposed to the measured value in air. The behavior of  $\mu^-$  in the detector would also be an interesting study to apply to future experiments. While these corrections were not possible with the information and technology presently available, their effects on future results would be interesting.

## References

---

- [1] H. Yukawa, *Proc. Phys. Math. Soc. Japan* **17**, 48 (1946).
- [2] C. Anderson and S. Nedermeyer, *Phys. Rev.* **50**, 263 (1936).
- [3] M. Conversi, E. Pancini, and Q. Piccioni, *Phys. Rev.* **71**, 209 (1947).
- [4] C. M. G. Lattes *et al.*, *Nature* **159**, 694 (1947).
- [5] E.J. Weinberg and D.L. Nordstrom, *Phys. Rev. D.* **54**, 250 (1996).
- [6] R.L. Garwin, L. M. Lederman, and M. Weinrich, *Phys. Rev.* **105**, 1415 (1957).
- [7] J. Bailey *et al.*, *Nucl Phys.* **B150**, 1 (1979).
- [8] H. N. Brown *et al.*, <http://arXiv.org/abs/hep-ex/0102017>, (Preprint; 2001).
- [9] A. Czarnecki, W.J. Marciano. <http://arXiv.org/abs/hep-ph/0102122>, (Preprint; 2001).
- [10] F. J. Ynduráin, <http://arXiv.org/abs/hep-ph/0102312>, (Preprint; 2001).
- [11] M. Hayakawa, T. Kinoshita, <http://arXiv.org/abs/hep-ph/0112102>, (Preprint; 2001).
- [12] C. Amsler, *Am. J. Phys.* **42**, 1067 (1974).
- [13] N. Easwar, D. A. MacIntire, *Am. J. Phys.* **59**, 7 (1991).
- [14] T. Ward *et al.* *Am. J. Phys.* **53**, 542 (1985).
- [15] Townsend, John S. *A Modern Approach to Quantum Mechanics*. (McGraw-Hill, New York, 1992), pp. 97-100.
- [16] F. James and M. Roos. MINUIT – *Function Minimization and Error Analysis*. Technical Report CERN Program Library Number D506, CERN, 1989.
- [17] R. Brun and F. Radermakers. ROOT, An Object-Oriented Data Analysis Framework. *Users Guide v3.1b*, June 2001.

# Appendix A

## Apparatus Diagrams

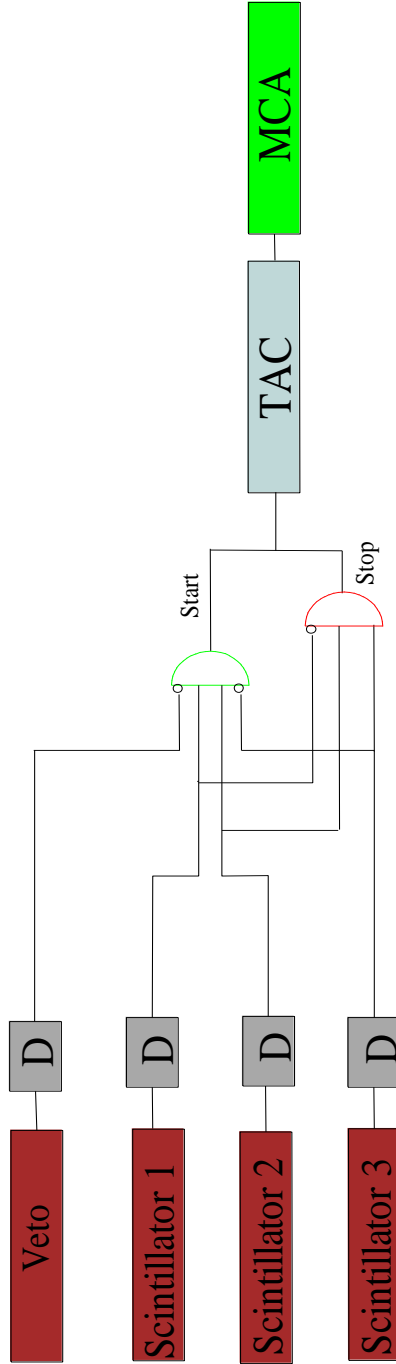


Figure 10: Scale Drawing of Apparatus.  
The detection apparatus consisted of three Bicron plastic scintillators inside of a solenoid. A fourth scintillator was placed outside of the field to veto events from nonuniform field regions.

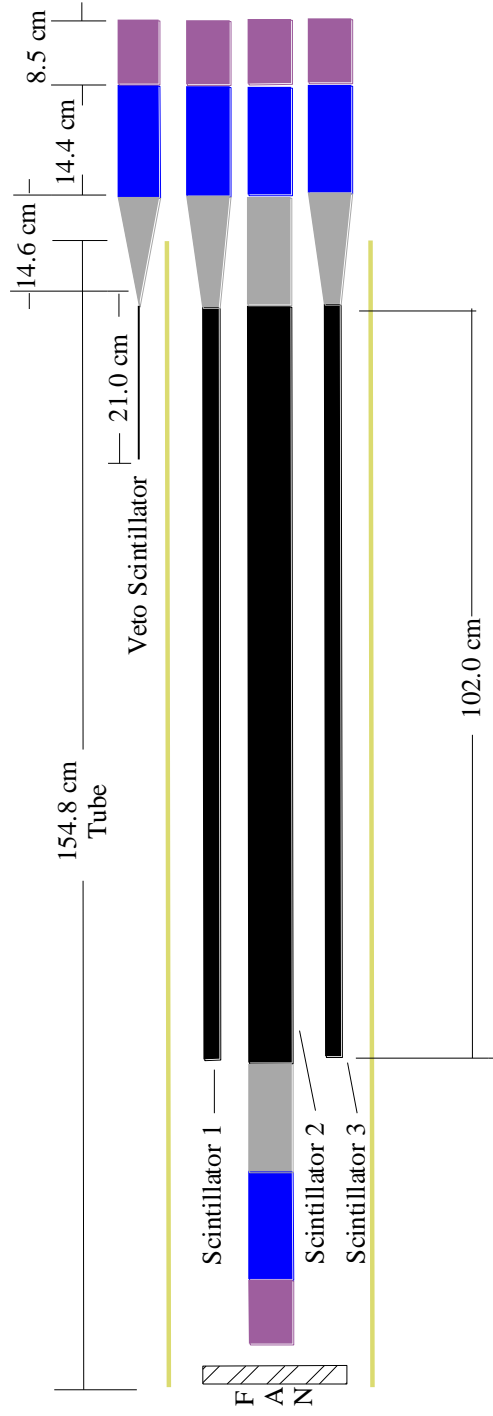


Figure 11: Electronics Diagram.  
 The Time to Amplitude Converter received a START pulse if a muon was detected by Scintillators 1 and 2, but not by Scintillator 3 or the veto. A STOP pulse was sent to the TAC if a signal (due to an exiting positron) was sent from Scintillators 2 and 3 but not Scintillator 1. If no STOP pulse was recorded the TAC would reset in 20  $\mu$ s. The time between the START and STOP pulse was converted by the TAC into an analog pulse with amplitude proportional to this time difference. The Multi-Channel Analyzer (MCA) then recorded the pulse from the TAC and binned the data appropriately.

## Appendix B

### Data Taken With Magnetic Field Off

Channel	Events	Channel	Events	Channel	Events	Channel	Events
1	0	38	414	75	294	112	261
2	0	39	430	76	327	113	275
3	0	40	453	77	310	114	240
4	0	41	389	78	296	115	220
5	0	42	432	79	305	116	231
6	0	43	450	80	286	117	266
7	0	44	438	81	304	118	225
8	0	45	385	82	323	119	246
9	0	46	410	83	323	120	191
10	3	47	397	84	288	121	208
11	516	48	404	85	306	122	178
12	572	49	382	86	296	123	243
13	545	50	435	87	273	124	196
14	596	51	402	88	290	125	199
15	533	52	417	89	287	126	218
16	509	53	358	90	286	127	208
17	528	54	379	91	277	128	215
18	542	55	394	92	281	129	195
19	541	56	369	93	297	130	200
20	547	57	395	94	274	131	213
21	539	58	383	95	271	132	206
22	526	59	386	96	274	133	202
23	485	60	362	97	253	134	210
24	479	61	379	98	231	135	232
25	482	62	359	99	276	136	173
26	485	63	361	100	248	137	199
27	467	64	402	101	262	138	191
28	495	65	357	102	278	139	183
29	491	66	353	103	276	140	181
30	477	67	358	104	280	141	186
31	463	68	366	105	238	142	183
32	458	69	347	106	221	143	197
33	484	70	336	107	241	144	178
34	474	71	340	108	232	145	180
35	458	72	351	109	225	146	162
36	461	73	341	110	207	147	159
37	445	74	308	111	232	148	169

149	167	195	102	241	68	287	76
150	202	196	116	242	101	288	64
151	176	197	102	243	83	289	64
152	155	198	135	244	93	290	57
153	147	199	123	245	63	291	48
154	165	200	109	246	84	292	58
155	172	201	117	247	90	293	58
156	133	202	124	248	81	294	63
157	138	203	95	249	82	295	51
158	143	204	139	250	96	296	66
159	156	205	100	251	67	297	49
160	166	206	107	252	71	298	69
161	178	207	96	253	57	299	50
162	141	208	106	254	76	300	57
163	158	209	103	255	74	301	46
164	162	210	114	256	69	302	61
165	173	211	94	257	68	303	74
166	155	212	107	258	72	304	57
167	132	213	111	259	80	305	49
168	143	214	89	260	72	306	41
169	127	215	122	261	71	307	52
170	162	216	110	262	75	308	43
171	134	217	93	263	65	309	49
172	150	218	110	264	67	310	57
173	127	219	95	265	73	311	71
174	135	220	99	266	81	312	51
175	138	221	85	267	75	313	49
176	139	222	90	268	75	314	69
177	126	223	96	269	73	315	57
178	137	224	100	270	56	316	40
179	130	225	94	271	75	317	47
180	113	226	87	272	68	318	65
181	137	227	98	273	66	319	46
182	130	228	75	274	72	320	49
183	124	229	85	275	71	321	52
184	126	230	81	276	65	322	36
185	107	231	88	277	67	323	52
186	110	232	84	278	59	324	49
187	134	233	81	279	62	325	54
188	124	234	68	280	68	326	42
189	128	235	108	281	50	327	43
190	116	236	76	282	57	328	47
191	137	237	78	283	57	329	42
192	109	238	76	284	53	330	39
193	124	239	71	285	66	331	34
194	102	240	78	286	56	332	50

333	53	377	32	421	30	465	30
334	40	378	31	422	33	466	21
335	39	379	40	423	27	467	23
336	45	380	30	424	23	468	23
337	47	381	30	425	25	469	29
338	42	382	36	426	25	470	25
339	46	383	28	427	29	471	19
340	42	384	37	428	19	472	27
341	42	385	33	429	24	473	33
342	48	386	40	430	25	474	18
343	35	387	36	431	23	475	23
344	38	388	32	432	32	476	26
345	46	389	27	433	30	477	23
346	43	390	20	434	22	478	21
347	31	391	32	435	26	479	24
348	51	392	30	436	24	480	18
349	42	393	42	437	18	481	24
350	53	394	33	438	25	482	22
351	42	395	28	439	27	483	19
352	28	396	30	440	17	484	21
353	48	397	26	441	17	485	27
354	49	398	35	442	17	486	21
355	52	399	41	443	25	487	24
356	35	400	25	444	35	488	25
357	42	401	27	445	22	489	22
358	41	402	34	446	25	490	22
359	35	403	25	447	25	491	26
360	25	404	26	448	20	492	21
361	34	405	23	449	23	493	21
362	46	406	29	450	23	494	22
363	18	407	29	451	30	495	17
364	39	408	29	452	24	496	20
365	36	409	33	453	18	<b>Total</b>	67329
366	33	410	28	454	23	<b>Number</b>	
367	32	411	33	455	26	<b>of Events</b>	
368	39	412	31	456	22		
369	41	413	32	457	27		
370	34	414	26	458	33		
371	32	415	25	459	22		
372	39	416	24	460	26		
373	37	417	34	461	28		
374	36	418	38	462	17		
375	39	419	29	463	25		
376	35	420	22	464	32		



## Data Taken With Magnetic Field On

Channel	Events	Channel	Events	Channel	Events	Channel	Events
1	0	40	459	79	330	118	236
2	0	41	455	80	313	119	207
3	2	42	416	81	297	120	206
4	0	43	417	82	315	121	213
5	1	44	432	83	289	122	204
6	3	45	389	84	310	123	215
7	1	46	444	85	315	124	208
8	4	47	425	86	336	125	215
9	2	48	425	87	308	126	234
10	65	49	434	88	283	127	194
11	583	50	370	89	288	128	211
12	636	51	402	90	272	129	202
13	584	52	380	91	288	130	215
14	583	53	362	92	276	131	207
15	597	54	368	93	294	132	193
16	563	55	377	94	253	133	184
17	525	56	372	95	273	134	189
18	562	57	364	96	272	135	187
19	561	58	397	97	265	136	190
20	550	59	366	98	272	137	181
21	518	60	340	99	248	138	196
22	558	61	331	100	234	139	199
23	537	62	374	101	286	140	180
24	539	63	334	102	240	141	176
25	498	64	338	103	209	142	170
26	492	65	327	104	265	143	192
27	494	66	362	105	228	144	192
28	534	67	332	106	219	145	183
29	469	68	331	107	246	146	166
30	473	69	349	108	220	147	195
31	482	70	331	109	249	148	155
32	488	71	361	110	230	149	164
33	487	72	352	111	235	150	170
34	457	73	320	112	239	151	188
35	478	74	329	113	238	152	180
36	504	75	328	114	241	153	166
37	424	76	315	115	228	154	190
38	444	77	340	116	214	155	149
39	439	78	372	117	215	156	155

157	164	203	116	249	87	295	48
158	150	204	120	250	73	296	60
159	154	205	123	251	63	297	42
160	144	206	114	252	82	298	46
161	148	207	106	253	73	299	64
162	146	208	109	254	76	300	47
163	160	209	120	255	77	301	44
164	137	210	93	256	79	302	42
165	149	211	102	257	72	303	64
166	131	212	85	258	76	304	55
167	145	213	115	259	83	305	45
168	127	214	118	260	50	306	51
169	157	215	109	261	85	307	57
170	151	216	92	262	94	308	55
171	135	217	81	263	79	309	60
172	154	218	94	264	80	310	42
173	139	219	86	265	69	311	51
174	140	220	93	266	56	312	52
175	138	221	108	267	65	313	46
176	125	222	102	268	77	314	46
177	130	223	102	269	79	315	60
178	122	224	103	270	59	316	43
179	139	225	86	271	70	317	51
180	125	226	115	272	54	318	41
181	133	227	105	273	70	319	56
182	138	228	98	274	56	320	47
183	110	229	84	275	78	321	48
184	127	230	77	276	75	322	41
185	122	231	99	277	58	323	58
186	124	232	77	278	83	324	48
187	119	233	81	279	67	325	37
188	120	234	80	280	70	326	46
189	132	235	99	281	66	327	44
190	117	236	86	282	65	328	41
191	139	237	74	283	62	329	50
192	112	238	101	284	71	330	43
193	92	239	81	285	45	331	38
194	110	240	77	286	63	332	33
195	132	241	74	287	54	333	44
196	126	242	79	288	61	334	54
197	110	243	80	289	56	335	44
198	101	244	80	290	57	336	44
199	115	245	70	291	47	337	42
200	112	246	102	292	57	338	48
201	126	247	86	293	51	339	45
202	103	248	77	294	57	340	38

341	40	381	32	421	23	461	23
342	42	382	34	422	24	462	20
343	42	383	40	423	17	463	26
344	34	384	32	424	17	464	24
345	41	385	40	425	26	465	23
346	40	386	28	426	21	466	25
347	38	387	32	427	28	467	16
348	54	388	31	428	29	468	26
349	48	389	28	429	20	469	22
350	36	390	29	430	31	470	18
351	44	391	33	431	28	471	26
352	40	392	36	432	17	472	21
353	35	393	32	433	29	473	29
354	39	394	25	434	30	474	27
355	26	395	27	435	18	475	19
356	30	396	30	436	19	476	29
357	42	397	27	437	24	477	21
358	39	398	30	438	19	478	23
359	25	399	26	439	35	479	24
360	37	400	28	440	28	480	17
361	47	401	36	441	32	481	26
362	36	402	30	442	24	482	29
363	35	403	29	443	25	483	20
364	34	404	26	444	24	484	26
365	25	405	25	445	34	485	21
366	31	406	28	446	22	486	13
367	32	407	23	447	34	487	22
368	36	408	38	448	18	488	19
369	25	409	24	449	25	489	20
370	32	410	23	450	25	490	15
371	36	411	26	451	21	491	14
372	33	412	21	452	24	492	19
373	24	413	30	453	20	493	29
374	31	414	36	454	23	494	35
375	36	415	37	455	27	495	19
376	28	416	43	456	30	496	20
377	31	417	27	457	28	<b>Total</b>	<b>67593</b>
378	36	418	38	458	19	<b>Number</b>	
379	27	419	26	459	22	<b>of Events</b>	
380	34	420	28	460	28		

## Appendix C

### Root Code Used for Plotting and Fitting the Decay Curves

```
gROOT.Reset ("a");

#include <iostream.h>
#include <fstream.h>
#include "TMinuit.h"

Float_t chan[550], time[550], counts[550],error[550];
Float_t fitcounts1[550],fitcounts2[550],fittime[550];
Float_t errorx[550]=0.;
Int_t lowchan=100;
Int_t hichan=400;
Int_t bin=10;
Int_t nchan = (hichan-lowchan)/bin;      // number of channels in spectrum

Float_t calib1=0.0193548;
Float_t calib2=0.;

//=====
==

void
fcn (Int_t & npar, Double_t *gin, Double_t & f, Double_t *par, Int_t iflag)
{
    Int_t i;

    // calculate chisquare
    Double_t chisq = 0.;
    Double_t delta = 0.;

    for (i = 0; i < nchan; i++)

    {
        if (error[i] != 0.) then
        {
            delta = (counts[i]-func(time[i],par))/error[i];
            chisq += delta*delta;
        }
    }

    f = chisq;
}

//=====
==
Double_t
func (float ttime, Double_t * par)
{
```

```

Double_t x = par[0]*exp(par[1] * (par[2]-ttime))*(1.+par[3]*cos(par[4]*ttime+par[5])) +par[6];
return x;
}

//=====
==
int
fit_to_decay ()

{
  Int_t i, k;
  Float_t temp, sum;

  // Read in the file
  TString *data_file = new TString("/home/public/muon_data/background2_15_02a.txt");
  cout<<data_file->Data()<<endl;

  ifstream istream (data_file->Data(), ios::in);

  k=0;
  for(i=0;i<=hichan;i+=bin)
  {
    sum = 0;

    for(j=0;j<bin;j++)
    {
      istream>>temp;
      sum = sum+temp;
    }

    if (i>=lowchan)
    {
      counts[k]=sum;
      chan[k]=i+bin/2.;
      time[k]=calib1*chan[k]+calib2;
      error[k]=sqrt(counts[k]);
      cout<<" nchan"<<nchan<<" i"<<i<<" k"<<k<<" time"<<time[k]<<" chan"<<chan[k]<<"
"<<counts[k]<<endl;
      k++;
    }
  }

  // Make the graph

  TCanvas *c1= new TCanvas ("c1","zzz",200,10,800,400);
  TGraph *gr1 = new TGraphErrors(nchan,time,counts,errorx,error);
  gr1->SetMarkerStyle(21);
  gr1->SetMarkerSize(0.5);
  gr1->Draw("AP");

  // Initialize TMinuit with a maximum of 4 params
  TMinuit *gMinuit = new TMinuit (8);

```

```

gMinit->SetFCN (fcn);

    Double_t arglist[10];
    Int_t ierflg = 0;

/* SET ERRordef <up>
   Sets the value of UP (default value= 1.), defining parameter
   errors. Minit defines parameter errors as the change
   in parameter value required to change the function value
   by UP. Normally, for chisquared fits UP=1, and for negative
   log likelihood, UP=0.5. */
arglist[0] = 1.;
gMinit->mnexcm ("SET ERR", arglist, 1, ierflg);

// Set starting values and step sizes for parameters
Double_t vstart[7] = { 2500.,0.5,0.,0.04,5.,0.1,1000. };
Double_t step[7] = { 0.01, 0.01, 0.01,0.01, 0.01, 0.01,0.01 };
gMinit->mnparm (0, "Norm", vstart[0], step[0], 400., 20000., ierflg);
gMinit->mnparm (1, "Decay", vstart[1], step[1], 0., 1., ierflg);
gMinit->mnparm (2, "Shift", vstart[2], step[2], -1.,1., ierflg);
gMinit->mnparm (3, "Ncos", vstart[3], step[3], -10.,10., ierflg);
gMinit->mnparm (4, "Omega", vstart[4], step[4], 0.,100., ierflg);
gMinit->mnparm (5, "Phase", vstart[5], step[5], -100.,100., ierflg);
gMinit->mnparm (6, "Bkgd", vstart[6], step[6], 0., 5000., ierflg);

// Now ready for minimization step
arglist[0] = 500.;
arglist[1] = 1.;
Double_t p1 = 1;
Double_t p2 = 2;
Double_t p3 = 3;
Double_t p4 = 4;
    Double_t p5 = 5;
Double_t p6 = 6;
Double_t p7 = 7;

gMinit->mnexcm ("RELEASE", &p1, 1, ierflg);
gMinit->mnexcm ("RELEASE", &p2, 1, ierflg);
gMinit->mnexcm ("FIX", &p3, 1, ierflg);
gMinit->mnexcm ("FIX", &p4, 1, ierflg);
gMinit->mnexcm ("FIX", &p5, 1, ierflg);
gMinit->mnexcm ("FIX", &p6, 1, ierflg);
gMinit->mnexcm ("FIX", &p7, 1, ierflg);
gMinit->mnexcm ("MIGRAD", arglist, 2, ierflg);

gMinit->mnexcm ("FIX", &p1, 1, ierflg);
gMinit->mnexcm ("FIX", &p2, 1, ierflg);
gMinit->mnexcm ("RELEASE", &p3, 1, ierflg);
gMinit->mnexcm ("FIX", &p4, 1, ierflg);
gMinit->mnexcm ("FIX", &p5, 1, ierflg);
gMinit->mnexcm ("FIX", &p6, 1, ierflg);
gMinit->mnexcm ("RELEASE", &p7, 1, ierflg);
gMinit->mnexcm ("MIGRAD", arglist, 2, ierflg);

```

```

gMinit->mnexcm ("RELEASE", &p1, 1, ierflg);
gMinit->mnexcm ("RELEASE", &p2, 1, ierflg);
gMinit->mnexcm ("RELEASE", &p3, 1, ierflg);
gMinit->mnexcm ("FIX", &p4, 1, ierflg);
gMinit->mnexcm ("FIX", &p5, 1, ierflg);
gMinit->mnexcm ("FIX", &p6, 1, ierflg);
gMinit->mnexcm ("RELEASE", &p7, 1, ierflg);
gMinit->mnexcm ("MIGRAD", arglist, 2, ierflg);

```

```

gMinit->mnexcm ("FIX", &p1, 1, ierflg);
gMinit->mnexcm ("FIX", &p2, 1, ierflg);
gMinit->mnexcm ("FIX", &p3, 1, ierflg);
gMinit->mnexcm ("FIX", &p4, 1, ierflg);
gMinit->mnexcm ("RELEASE", &p5, 1, ierflg);
gMinit->mnexcm ("RELEASE", &p6, 1, ierflg);
gMinit->mnexcm ("FIX", &p7, 1, ierflg);
gMinit->mnexcm ("MIGRAD", arglist, 2, ierflg);

```

```

gMinit->mnexcm ("FIX", &p1, 1, ierflg);
gMinit->mnexcm ("FIX", &p2, 1, ierflg);
gMinit->mnexcm ("FIX", &p3, 1, ierflg);
gMinit->mnexcm ("RELEASE", &p4, 1, ierflg);
gMinit->mnexcm ("FIX", &p5, 1, ierflg);
gMinit->mnexcm ("FIX", &p6, 1, ierflg);
gMinit->mnexcm ("FIX", &p7, 1, ierflg);
gMinit->mnexcm ("MIGRAD", arglist, 2, ierflg);

```

```

gMinit->mnexcm ("RELEASE", &p1, 1, ierflg);
gMinit->mnexcm ("RELEASE", &p2, 1, ierflg);
gMinit->mnexcm ("RELEASE", &p3, 1, ierflg);
gMinit->mnexcm ("RELEASE", &p4, 1, ierflg);
gMinit->mnexcm ("RELEASE", &p5, 1, ierflg);
gMinit->mnexcm ("RELEASE", &p6, 1, ierflg);
gMinit->mnexcm ("RELEASE", &p7, 1, ierflg);
gMinit->mnexcm ("MIGRAD", arglist, 2, ierflg);

```

```

// Print results
Double_t amin,edm,errdef;
Int_t nvar,nparx,icstat;
gMinit->mnstat(amin,edm,errdef,nvar,nparx,icstat);
gMinit->mnprin(3,amin);

```

```

//Plot Results

Double_t ppar[7], epar[7];
cout<<endl<<endl<<"Final Parameters:"<<endl;
for (Int_t i = 0; i < 7; i++)
{
gMinit.GetParameter (i, ppar[i], epar[i]);
cout << i<<" "<<ppar[i] <<" "<< epar[i] << endl;
}

k=0;

```

```

    for (i=lowchan; i<hichan; i++)
        {
            fittime[k]=calib1*i+calib2;
            fitcounts1[k] = func (fittime[k], ppar);
            k++;
        }

    k=0;
    ppar[3]=0.;
    for (i=lowchan; i<hichan; i++)
        {
            fittime[k]=calib1*i+calib2;
            fitcounts2[k] = func (fittime[k], ppar);
            k++;
        }

    TGraph *gr2 = new TGraph(hichan-lowchan,fittime,fitcounts1);
    gr2->SetMarkerStyle(21);
    gr2->SetMarkerSize(0.);
    gr2->Draw("L");

    //TGraph *gr3 = new TGraph(hichan-lowchan,fittime,fitcounts2);
    //gr3->SetMarkerStyle(21);
    //gr3->SetMarkerSize(0.);
    //gr3->Draw("L");

    return(1);
}

```